Capillary Waves at the Transition from Propagating to Overdamped Behavior

A. Madsen,[1,*] T. Seydel,[2] M. Sprung,[3] C. Gutt,[3] M. Tolan,[3] and G. Grübel[1]

[1]*European Synchrotron Radiation Facility, BP 220, F-38043 Grenoble, France*

[2]*Institut Laue-Langevin, BP 156, F-38042 Grenoble, France*

[3]*Experimentelle Physik 1, Universität Dortmund, Otto-Hahn-Strasse 4, D-44221 Dortmund, Germany*

(Received 23 June 2003; published 4 March 2004)

We measure the dispersion relation of capillary waves on a liquid surface by heterodyne x-ray photon correlation spectroscopy near the transition from propagating to overdamped dynamic behavior. A strong deviation of the propagation frequency from the small-damping result $\omega_p \propto k^{3/2}$ is observed long before the actual transition where $(\partial\omega_p/\partial k) < 0$ and ω_p tends to zero. This behavior is successfully described by expressions derived within linear response theory.

DOI: 10.1103/PhysRevLett.92.096104 PACS numbers: 68.03.Kn, 61.10.–i

Every liquid surface is subject to fluctuating displacements caused by thermally activated capillary waves [1]. Capillary waves are harmonic waves with the surface tension acting as a restoring force and their presence has indirectly been verified by diffuse x-ray scattering and reflectivity measurements on the surface of various liquids [2–5]. The value of the measured roughness exceeds the intrinsic roughness caused by the liquid molecule size and hence yields an indirect proof of a height disturbance that makes the surface fuzzy. However, such roughness measurements are time averaged and cannot reveal the dynamic behavior of the waves. To probe the dynamics, photon correlation spectroscopy experiments have been performed with visible laser light on various liquids, gels, and polymer solutions [6–9]. A capillary wave is identified by its wave vector k and complex frequency $f = \omega_p + i\Gamma$, where the real part reflects the propagation frequency and the imaginary part the damping. The wave can be either propagating or overdamped depending on k, the surface tension σ, the dynamic viscosity η, and the density ρ of the liquid. On a simple liquid surface the propagating modes become unstable as the damping is increased and at the transition from propagating to overdamped behavior f becomes purely imaginary; i.e., $\omega_p = 0$. Such a crossover from inelastic to quasielastic behavior has also been predicted within the two-fluid model by Harden *et al.* [10] for systems with marked elastic properties and observed by light scattering in gel and polymer systems [9]. Recently, the coexistence of elastic Rayleigh modes and usual capillary modes has been reported when a soft-gel surface is electrically excited [11]. In the work reported here, we study the dynamics of thermally activated capillary waves near the transition from propagating to overdamped behavior by x-ray photon correlation spectroscopy (XPCS) [12–16] in a mixture of water and glycerol. Glycerol is a prototypical glass forming liquid and its viscosity increases rapidly upon cooling [5,12]. Hence, by tuning the temperature it is possible to observe the crossover from propagating to overdamped waves in the experimentally accessible q range. The aim of this work is to study the dispersion relation of capillary waves in the vicinity of this transition.

For the experiments we prepared a sample as a mixture of water and glycerol with 65% weight concentration of glycerol. Glycerol is a hygroscopic liquid and fully miscible with water. The sample had a large flat surface and was kept in a trough in an evacuated sample cell which is described in detail in Ref. [15]. The cell provides accurate control of the sample temperature through a combination of a resistive heater and a cryogenic cooling device controlled by a feedback system. The residual gas pressure above the surface was some tens of millibars determined by the vapor pressure of the liquid. By x-ray reflectometry it was verified that the sample did not phase separate nor exhibited any layering effects. The XPCS measurements were performed at the TROÏKA beam line ID10A of the European Synchrotron Radiation Facility with an x-ray energy of 8.05 keV ($\lambda = 1.54$ Å) selected by a single bounce Si(111) monochromator operating in horizontal scattering geometry. By tilting the Si crystal the monochromatic beam was deflected down to impinge on a Pt coated quartz mirror. The incident angle on the mirror was chosen such that higher order light was suppressed in the reflected beam. By a proper collimation employing two slit assemblies (upstream of the monochromator) and a 10 μm pinhole aperture inserted in the monochromatic beam after the mirror, the beam was made (partially) coherent. Parasitic scattering from the pinhole was removed by careful positioning of a guard slit. The beam reflected from the mirror was directed down towards the horizontal sample surface. The incidence angle α_i of the coherent x-ray beam was kept constant at 0.1°, which is below the critical angle of total external reflection. In this case, the $1/e$ penetration depth of the evanescent wave in the sample is around 100 Å making the experiment highly surface sensitive. The momentum transfer parallel to the surface is given by $q = 2\pi(\cos\alpha_i - \cos\alpha_f)/\lambda$ and could be varied by changing α_f, the takeoff angle of the beam scattered into the detector ($\alpha_f > \alpha_i$, vertical

scattering plane). Scattered photons were detected by a fast avalanche photo diode (APD) and the output signal from the APD was processed online by a FLEX autocorrelator from Correlator.com™ to calculate the time-correlation function $g(\tau)$ at the given q.

Figure 1 displays three correlation functions taken at the same q but at different temperatures, 5, 12, and 30 °C, respectively. While the high temperature correlation function clearly shows an oscillating behavior, characteristic for propagating capillary waves, the low temperature data follow an exponential decay indicating overdamped waves. For the intermediate temperature this distinction is not obvious. In grazing incidence surface XPCS experiments an optical mixing takes place close to the specular reflected beam (i.e., for small scattering vectors q parallel to the surface) [16]. Hence, the measured time-correlation function $g(q, \tau)$ is obtained as a combination of heterodyne and homodyne terms and

$$g(q, \tau) = \alpha \mathrm{Re}\{g_1(q, \tau)\} + \beta g_2(q, \tau) + \gamma, \qquad (1)$$

where α, β, and γ are q-dependent (but time-independent) functions and $g_1(q, \tau)$, $g_2(q, \tau)$ are the first and second order correlation functions of the surface fluctuation spectrum [16]. If the reference signal (specular reflection) is very intense compared to the diffuse scattered signal, the heterodyne term g_1 in Eq. (1) may be dominating, and this is the case in grazing incidence geometry [16]. $g_1(q, \tau)$ equals $\tilde{S}(q, \tau)$, the time Fourier transform of the dynamic structure factor of the surface, and if $S(q, \omega)$ is a simple Lorentzian which peaks at $\omega = \omega_0$ with a HWHM of Γ_0, then $\mathrm{Re}\{g_1(q, \tau)\} = \exp(-\Gamma_0 \tau)\cos(\omega_0 \tau)$. This holds in the limit of small damping (low viscosity and/or small q). However, in general $S(q, \omega)$ cannot be regarded as a simple Lorentzian, and thus the correlation function takes a more complicated form. To determine the dynamic structure factor all taken correlation functions were inverse Fourier transformed and the fitted peak position and width (HWHM) of $S(q, \omega)$ define the propagation frequency ω_p and damping constant Γ of the waves. In the following we concentrate on the measurements at 30 and 12 °C. The data taken at $T = 30$ °C all indicate propagating waves ($\omega_p \neq 0$) and in Fig. 2(a) the extracted values of ω_p (circles) and Γ (squares) are shown versus q. The dashed lines show the dispersion relations $\omega_0 = q^{3/2}\sqrt{\sigma/\rho}$ and $\Gamma_0 = 2\eta q^2/\rho$ valid for the propagation frequency and damping constant in the limit of small damping [1]. These expressions do not model the data very well. The agreement between the small-damping-limit model and the data taken at lower temperatures is even worse. Figure 2(b) shows data taken at $T = 12$ °C and in striking contrast to the model prediction (dashed lines) the measured propagation frequency (circles) falls to zero at approximately $q = 8 \times 10^{-6}$ Å^{-1}. This is

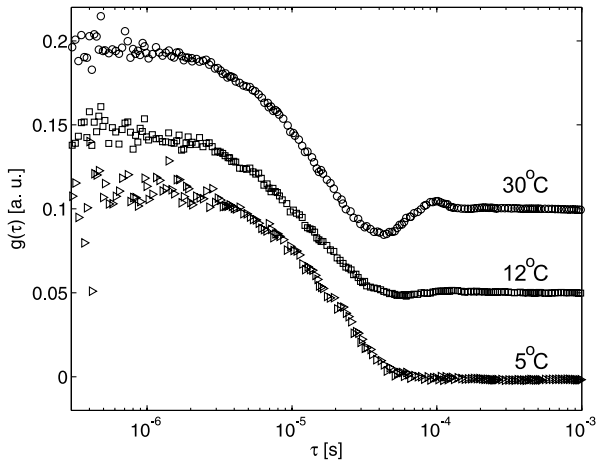

FIG. 1. Time-correlation functions of the scattered intensity at $q = 5.6 \times 10^{-6}$ Å^{-1} taken at different temperatures. The data have been shifted along the ordinate.

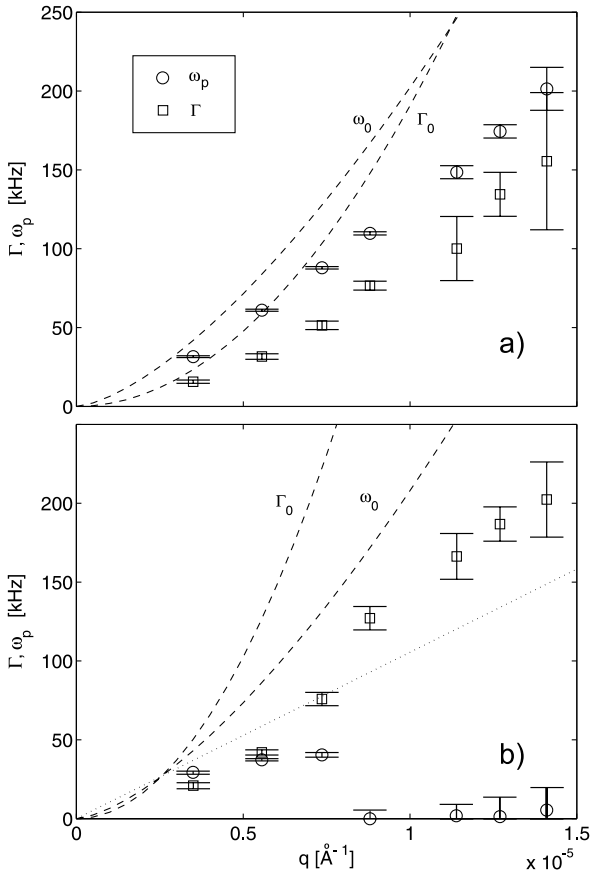

FIG. 2. Experimentally determined dispersion relations of the propagation frequency ω_p (circles) and the damping constant Γ (squares) for the water/glycerol mixture at (a) 30 °C and (b) 12 °C. The data deviate significantly from the small-damping expressions $\omega_0 = q^{3/2}\sqrt{\sigma/\rho}$ and $\Gamma_0 = 2\eta q^2/\rho$ [$\eta = 9.1$ cP, $\sigma = 0.047$ N/m, $\rho = 1156$ kg/m^3 (30 °C) and $\eta = 23.7$ cP, $\sigma = 0.050$ N/m, $\rho = 1156$ kg/m^3 (12 °C)] at both temperatures. At $T = 12$ °C a crossover ($\omega_p = 0$) is evident at $q \approx 8 \times 10^{-6}$ Å^{-1}. In the overdamped region ($q > 8 \times 10^{-6}$ Å^{-1}) a clear offset of the data (squares) from the strong-damping result $\Gamma = \sigma q/(2\eta)$ (dotted line) is observed in (b).

indicative of a transition from propagating to overdamped behavior of the capillary waves. The dotted line in Fig. 2(b) shows the dispersion relation $\Gamma = \sigma q/(2\eta)$ derived in the strong-damping limit [1]. Obviously, this limit neither applies since it clearly underestimates the measured damping constant Γ (squares) for overdamped waves ($q > 8 \times 10^{-6}$ Å^{-1}).

To understand the complex behavior of the measured quantities $\omega_p(q)$ and $\Gamma(q)$ in this transition region we turn to linear response theory by which the response of a liquid surface to an external force may be evaluated. A calculation [17] of the dynamic susceptibility χ of vertical surface displacements for an incompressible viscoelastic medium, including the effect of gravity, yields $\chi(k, \omega) = k\rho^{-1}/D(k, \omega)$. Here, $D(k, \omega)$ is given by

$$D(k, \omega) = gk + \sigma k^3/\rho - (\omega + 2i\nu k^2)^2 - 4\nu^2 k^4[1 - i\omega/(\nu k^2)]^{1/2}, \quad (2)$$

where $\nu = \eta/\rho$ is the kinematic viscosity. According to the dissipation theorem, the spectrum of the surface fluctuations $S(k, \omega)$ (dynamic structure factor) is determined by the imaginary part of the susceptibility and one finds [17]

$$S(k, \omega) = -2k_B T \frac{k}{\rho\omega} \frac{\mathrm{Im}D(k, \omega)}{|D(k, \omega)|^2}. \quad (3)$$

This expression is equivalent to that derived by Bouchiat and Meunier [6] and by Loudon [18] in the absence of any bulk contribution. Jäckle and Kawasaki [17] discuss Eq. (3) in the case of small damping (propagating modes) where continuum theory is valid (small k) and the effect of gravity is negligible and find

$$S(k, \omega) = 8k_B T \frac{k^3}{\rho} \frac{\nu}{(\omega^2 - \omega_0^2)^2 + (4\omega\nu k^2)^2}, \quad (4)$$

where $\omega_0 = k^{3/2}\sqrt{\sigma/\rho}$ is the capillary wave propagation frequency in an ideal incompressible fluid in the limit of small damping. The damping constant can be estimated from Eq. (4) and in the small-damping limit the HWHM of the peak at $\omega = \omega_0$ is given by $\Gamma_0 = 2\eta k^2/\rho$ as anticipated. In the transition region from propagating to overdamped capillary waves that is considered here, the dispersion relation of the propagation frequency ω_p can be numerically approximated from Eq. (3) and we find

$$\omega_p \approx \tfrac{2}{3}\mathrm{Re}\{(\omega_0^2 - 5\nu^2 k^4/4)^{1/2}\}. \quad (5)$$

It is noteworthy that ω_p deviates from the limiting case ω_0 by a factor which is viscosity and wave-vector dependent, and hence one expects the relation $\omega_p(k) \propto k^{3/2}$ to break down gradually as the damping increases. The critical wave vector k_c at which the transition from propagating to overdamped waves takes place ($\omega_p = 0$) can be derived from Eq. (5) to give

$$k_c = \frac{4\sigma\rho}{5\eta^2}. \quad (6)$$

The k_c that we determine here is more than a factor of 2 smaller than previously estimated [1,7]. To illustrate this we have calculated $S(k, \omega)$ from Eq. (3) for a viscous liquid ($\rho = 1156$ kg/m^3, $\eta = 18.8$ cP, and $\sigma = 0.039$ N/m). The result for different wave vectors is shown in Fig. 3 and for all k values the spectrum $S(\omega)$ has a strong quasielastic component in addition to the inelastic Brillouin peak. At $k = k_c \approx 1 \times 10^{-5}$ Å^{-1} the Brillouin peak vanishes and the spectrum becomes quasielastic with a broad peak centered at $\omega = 0$. This indicates a transition from propagating (inelastic) to overdamped (quasielastic) behavior. The propagation frequency ω_p (circles) and the damping constant Γ (squares) derived from the calculated spectra are plotted as a function of k in the inset to Fig. 3 and strong deviations from the ω_0 and Γ_0 behaviors (dashed lines) are observed. ω_p reaches a maximum value of $\sim\sigma k_c/(5\eta)$ at $k = 3k_c/4$ after which $(\partial\omega_p/\partial k) < 0$ and decreases rapidly to zero at $k = k_c$ as predicted by Eq. (5) (solid line). In the strong-damping limit the damping constant is given by $\Gamma = \sigma k/(2\eta)$ shown as the dotted line in the inset to Fig. 3. For $k > 1 \times 10^{-5}$ Å^{-1} one observes a large offset between the dotted line and the square symbols showing that near the transition, in the overdamped regime the damping constant is indeed larger than expected from a simple extrapolation of the strong-damping result.

The result of the data analysis is illustrated in Fig. 4 for the two temperatures. At $T = 30\,^\circ$C the data are well modeled over the full q range by the above outlined linear response theory, and the best fit (solid lines) yields

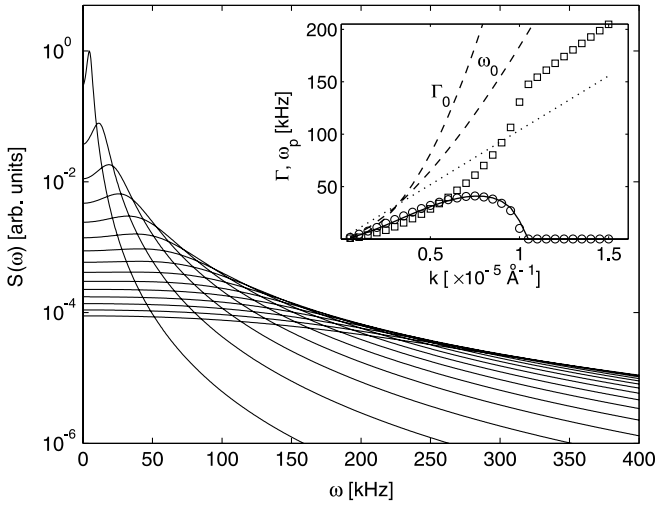

FIG. 3. The dynamic structure factor $S(q, \omega)$ calculated at $k = 1, 2, \ldots \times 10^{-6}$ Å^{-1} (top to bottom). The inset shows the crossover behavior of the center frequency ω_p (circles) and the HWHM Γ (squares) where ω_p is well described by Eq. (5) (solid line). The dashed lines in the inset show $\omega_0 = k^{3/2}\sqrt{\sigma/\rho}$ and $\Gamma_0 = 2\eta k^2/\rho$. The dotted line illustrates the strong-damping result $\Gamma = \sigma q/(2\eta)$.

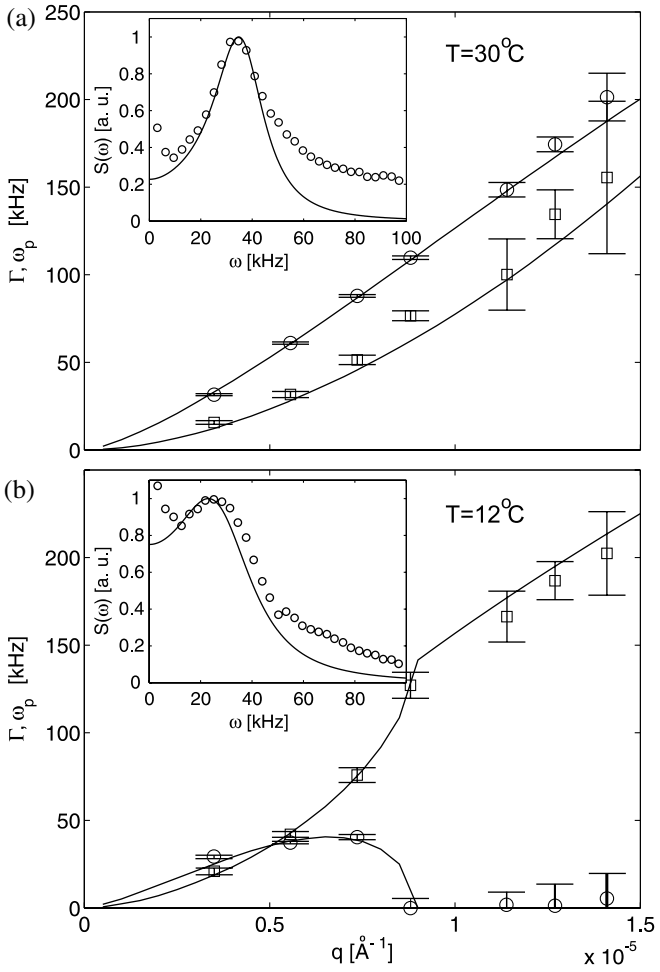

FIG. 4. Experimental data (from Fig. 2) that are well described by linear response theory (solid lines). The insets show inverse Fourier transformed time-correlation functions (circles) measured at 30 °C and 12 °C with $q = 3.5 \times 10^{-6}$ Å^{-1}, and the corresponding calculation of $S(\omega)$ (solid line) following Eq. (3).

the values $\eta = 9.1$ cP and $\sigma = 0.047$ N/m for the viscosity and surface tension. At $T = 12$ °C the measured crossover behavior is equally well reproduced by the model over the investigated q range. The best fit to ω_p with Eq. (5) yields $\eta = 23.7$ cP and $\sigma = 0.050$ N/m (solid line). This implies via Eq. (6) a critical wave vector $k_c = 8.2 \times 10^{-6}$ Å^{-1} in good agreement with the data. The crossover behavior is also evident from the measurements of Γ (squares) and the corresponding fit in Fig. 4(b) (solid line). At $q = k_c$ the behavior changes from $\Gamma \propto q^2$ to $\Gamma \propto q$ and the fit reproduces the data over the full q range within the error bars. The insets in Fig. 4 show selected inverse Fourier transformed time-correlation functions in the relevant ω range (circles). The solid lines in both insets are calculations of $S(\omega)$ following Eq. (3) using the above stated optimum fit values of η and σ. We believe that a small homodyne contribution to the correlation function and/or statistical noise is responsible for the deviations between the measurements and the calculated $S(\omega)$ spectra.

In summary we have measured the capillary wave dispersion relation on a liquid surface by heterodyne x-ray photon correlation spectroscopy in the transition region from propagating to overdamped modes. Long before the actual transition, strong deviations from the small-damping results occur. The data are well described by linear response theory and, in particular, the crossover behavior of the capillary wave propagation frequency ω_p close to k_c is well modeled by Eq. (5).

*Electronic address: amadsen@esrf.fr

[1] V. G. Levich, *Physicochemical Hydrodynamics* (Prentice-Hall, Englewood Cliffs, NJ, 1962).
[2] A. Braslau, M. Deutsch, P. S. Pershan, A. H. Weiss, J. Als-Nielsen, and J. Bohr, Phys. Rev. Lett. **54**, 114 (1985).
[3] M. K. Sanyal, S. K. Sinha, K. G. Huang, and B. M. Ocko, Phys. Rev. Lett. **66**, 628 (1991).
[4] B. M. Ocko, X. Z. Wu, E. B. Sirota, S. K. Sinha, and M. Deutsch, Phys. Rev. Lett. **72**, 242 (1994).
[5] T. Seydel, M. Tolan, B. M. Ocko, O. H. Seeck, R. Weber, E. DiMasi, and W. Press, Phys. Rev. B **65**, 184207 (2002).
[6] M. A. Bouchiat and J. Meunier, J. Phys. (Paris) **32**, 561 (1971).
[7] D. Byrne and J. C. Earnshaw, J. Phys. D **12**, 1133 (1979).
[8] *Light Scattering by Liquid Surfaces and Complementary Techniques*, edited by D. Langevin (Marcel Dekker, New York, 1992).
[9] R. B. Dorshow and L. A. Turkevich, Phys. Rev. Lett. **70**, 2439 (1993); H. Kikuchi, K. Sakai, and K. Takagi, Phys. Rev. B **49**, 3061 (1994).
[10] J. L. Harden, H. Pleiner, and P. A. Pincus, Langmuir **5**, 1436 (1989); J. Chem. Phys. **94**, 5208 (1991).
[11] F. Monroy and D. Langevin, Phys. Rev. Lett. **81**, 3167 (1998); K. Ahn, K. H. Yoon, and M.W. Kim, Europhys. Lett. **54**, 199 (2001).
[12] T. Seydel, A. Madsen, M. Tolan, G. Grübel, and W. Press, Phys. Rev. B **63**, 073409 (2001).
[13] H. J. Kim, A. Rühm, L. B. Lurio, J. Basu, J. Lal, D. Lumma, S. G. J. Mochrie, and S. K. Sinha, Phys. Rev. Lett. **90**, 068302 (2003).
[14] A. Madsen, J. Als-Nielsen, and G. Grübel, Phys. Rev. Lett. **90**, 085701 (2003).
[15] T. Seydel, A. Madsen, M. Sprung, M. Tolan, G. Grübel, and W. Press, Rev. Sci. Instrum. **74**, 4033 (2003).
[16] C. Gutt, T. Ghaderi, V. Chamard, A. Madsen, T. Seydel, M. Tolan, M. Sprung, G. Grübel, and S. K. Sinha, Phys. Rev. Lett. **91**, 076104 (2003); **91**, 179902(E) (2003).
[17] J. Jäckle and K. Kawasaki, J. Phys. Condens. Matter **7**, 4351 (1995).
[18] R. Loudon, Proc. R. Soc. London, Ser. A **372**, 275 (1980).